Large-Scale Fabrication of Carbon Nanotube Probe Tips For Atomic Force Microscopy Critical Dimension Imaging Applications

ARTICLE · FEBRUARY 2004

Source: NTRS

8 AUTHORS, INCLUDING:

Alan M Cassell
NASA
139 PUBLICATIONS **10,517** CITATIONS
SEE PROFILE

Jun li
Harbin Institute of Technology
251 PUBLICATIONS **7,288** CITATIONS
SEE PROFILE

Jie Han
University of Southern California
107 PUBLICATIONS **7,464** CITATIONS
SEE PROFILE

NANO LETTERS

xxxx
Vol. 0, No. 0
A−H

Large-Scale Fabrication of Carbon Nanotube Probe Tips for Atomic Force Microscopy Critical Dimension Imaging Applications

Qi Ye,*,†,‡ Alan M. Cassell,†,‡ Hongbing Liu,‡ Kuo-Jen Chao,§ Jie Han,†,‡ and M. Meyyappan†

Center For Nanotechnology, NASA Ames Research Center, Moffett Field, California 94035, Integrated Nanosystems, Inc., NASA Research Park, Moffett Field, California 94035, and Charles Evans & Associates, 810 Kifer Road, Sunnyvale, California 94086

Received May 3, 2004; Revised Manuscript Received May 24, 2004

ABSTRACT

We report an innovative approach that combines nanopatterning and nanomaterials synthesis with traditional silicon micromachining technologies for large-scale fabrication of carbon nanotube (CNT) probe tips for atomic force microscopy imaging applications. Our batch fabrication process has produced 244 CNT probe tips per 4-in. wafer with control over the CNT location, diameter, length, orientation, and crystalline morphology. CNT probe tips with diameters ranging between 40 and 80 nm and lengths between 2 and 6 μm are found to be functional probe tips with no need for shortening. This reliable and true bottom-up wafer scale integration and fabrication process provides a new class of high performance nanoprobes. Preliminary AFM imaging results show that the CNT probe tips are strong, wear-resistant, and capable of high-resolution and critical-dimension imaging.

Carbon nanotubes (CNTs) and related nanostructures possess remarkable electrical, mechanical, and thermal properties.[1] They show tremendous promise in a wide variety of applications including chemical sensors, biosensors, electronics, interconnects, field emitters, and scanning probes.[2−6] The idea of using carbon nanotubes as nanoprobes in scanning probe microscopy was first introduced by Dai et al. in 1996.[6] The intrinsic nanometer scale diameter, high aspect ratio, and strong mechanical robustness of CNTs make them ideal for high lateral resolution imaging[7,8] and deep trench/via critical dimension imaging[9] in semiconductor in-line processing applications. CNT probes are also highly desired in biological and chemical applications[10−12] where gentle probe−sample interactions are required. When CNT probes approach the sample surface during AFM tapping mode imaging, the CNT buckles elastically, which restricts the maximum force that can be applied to soft samples. CNT tips can also be functionalized at the tube open ends.[13,14] They can be made into multipurpose nanoprobes by imaging and sensing at the same time, and probing and manipulating materials at the same time. Therefore, CNT probes may be the ultimate probing tips for AFM.

Realizing the unique advantages of CNT probes, many efforts have been made to fabricate CNT-based imaging probes. Most reported work so far has relied on a "pick and stick" approach to manually attach multiwall CNTs on silicon pyramid tips under an optical microscope.[6−12] To improve this approach, an electric field has been applied to move multiwall CNTs on a conducting film to a silicon pyramid tip.[15] However, these approaches are tedious manual assembly processes and can fabricate CNT tips only one at a time. Advances have been made by direct catalytic growth of CNTs on silicon pyramid tips using thermal chemical vapor deposition (CVD) methods, either through coating catalysts all over the silicon pyramids or through creating nanopores on top of the flattened silicon pyramid tips.[16−18] Wafer scale production of CNT probe tips have also been attempted.[19,20] These approaches have scaled up the CNT tip fabrication processes and increased the fabrication throughput. However, thermal CVD growth has little control over the CNT location, density, length, and orientation. It is extremely difficult to obtain individual free-standing and well-oriented multiwall CNTs using thermal CVD. Readily usable tip yields are very low. In addition, these processes

* Corresponding author: Phone: (650) 604-0497, Fax: (650) 604-0987, E-mail: qye@mail.arc.nasa.gov
† NASA Ames Research Center.
‡ Integrated Nanosystems, Inc., NASA Research Park.
§ Charles Evans & Associates.

10.1021/nl049341r CCC: $27.50
Published on Web 00/00/0000

all rely on commercially available silicon tips or prefabricated commercial silicon probe wafers. At the end of the fabrication, these processes still require a one-at-a-time manipulation approach to remove extra CNTs and/or to shorten the remaining CNTs for tip use. To solve the problems that exist with current methodologies for making CNT-based imaging probes, we have developed an innovative bottom-up wafer scale fabrication method for the reliable mass fabrication of CNT probe tips through integration of nanopatterning and nanomaterials synthesis with traditional silicon cantilever microfabrication technology.

The key hurdle in nanoscience and nanotechnology is the integration of nanoscale materials with micron scale electronics and structures to form workable devices and sensors. Although there are numerous works discussing the growth, structures, and related unique properties of nanomaterials, studies addressing the issue of nano−micro integration for device and sensor fabrication have been scarce. We demonstrate here an example of integrating CNTs with silicon cantilevers for reliable fabrication of CNT based probe tips at wafer scale for AFM imaging applications. In this case, the nano−micro integration is achieved through catalyst nanopatterning and registration at wafer scale and through effective nanocatalyst protection and release before and after microfabrication. Our wafer scale fabrication method provides CNT tips that are directly grown from the silicon cantilevers at the wafer scale, not manually attached or randomly grown. CNT tip locations and diameters are defined by e-beam lithography. CNT length, orientation, and crystalline quality are controlled by the plasma enhanced chemical vapor deposition (PECVD) method. In PECVD, an electric field is present in the plasma discharge to direct the nanotubes to grow and align parallel to the electric field. Due to the crystalline morphology of our PECVD-grown CNTs, there is no need in our process to conduct post-fabrication treatment to remove and/or to shorten the CNT tips. With effective catalyst protection schemes, this fabrication process is very similar to the conventional approach for fabricating wafer-scale silicon AFM probe tips. Process control is therefore feasible and the overall yield is greatly improved. This is a truly bottom-up wafer-scale CNT AFM probe fabrication approach.

Our approach consists of six major steps: (1) wafer-scale nanopatterning and registration; (2) catalyst deposition and protection; (3) silicon microfabrication of cantilevers; (4) protection scheme release; (5) directional growth of CNTs from silicon cantilevers using the PECVD method; and (6) CNT probe tip characterization, performance evaluation, and testing. Figure 1 shows the photographs of one of our CNT AFM probe tip wafers fabricated using this approach. Figure 1a is a photograph of a whole 4-in. wafer containing 244 CNT AFM cantilever probe tips. Figure 1b and 1c are 8 × 3 and 3 × 1 arrays of cantilevers on this 4-in. wafer. Each cantilever is 1.6 mm × 3.4 mm in size and is held to the silicon wafer frame by 10 μm thick Si tabs on three sides. The x and y repeating coordinates for this tapping mode cantilever design are 4.01 mm and 6.60 mm, respectively. The process flow for this wafer-scale fabrication process is

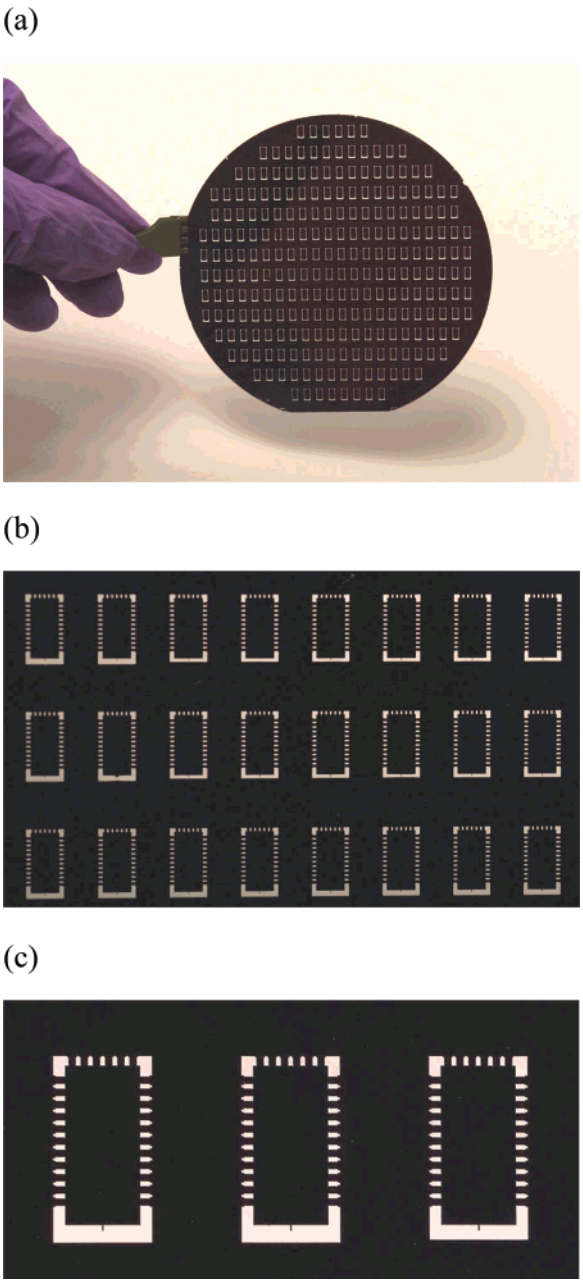

Figure 1. (a) Photograph of a 4-in. wafer containing 244 CNT AFM cantilever probe tips. (b) An 8 × 3 array of cantilevers on the 4-in. wafer. (c) Close look of the cantilevers, a 3 × 1 array on the 4-in. wafer. Each cantilever is 1.6 mm × 3.4 mm in size that is held to the silicon wafer frame by 10 μm thick Si tabs on three sides. The x and y repeating coordinates for this tapping mode cantilever design are 4.01 mm and 6.60 mm, respectively.

illustrated in Scheme 1. E-beam lithography is used to define the nanosized catalyst spots on whole wafers. A nitride protection layer and specialty protective chemicals are deposited on the front and back sides of wafers before microfabrication. Cantilevers are fabricated from silicon-on-insulator (SOI) wafers through a series of photolithographic patterning, dry, and wet etch process steps. CNT probe tips are grown at the end of the fabrication process from the defined catalyst spots on cantilever beams. The detailed wafer-scale fabrication process is described below step-by-step.

Scheme 1. Wafer-Scale Fabrication Process Flow for Making CNT AFM Probe Tips

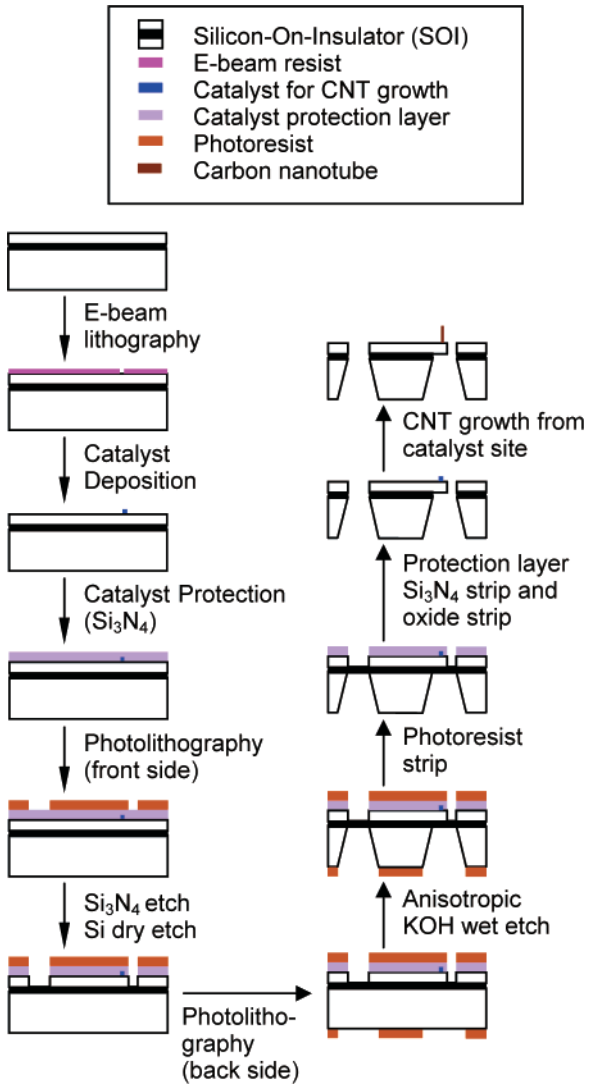

We used a high-speed electron beam writer Hitachi HL-700F e-beam system to pattern various catalyst feature sizes on a 4-in. SOI wafer (10 μm Si device layer, 1 μm oxide layer, and 380 μm Si handle layer). To investigate the optimal catalyst feature sizes for achieving single isolated CNT growth per catalyst site, we patterned catalyst dot sizes ranging from 50 to 300 nm in diameter with an interval of 50 nm. On a 4-in. SOI wafer, 244 dots were e-beam patterned for 244 cantilever tip locations at the end of the cantilever diving boards. As a control, we also patterned eight 1 μm catalyst sites at certain spots on the wafer. During the same e-beam lithography step, micron-scale global and local alignment marks were also patterned over the whole wafer to register these nanometer sized dot arrays. A highly sensitive bi-layer resist composed of low and high molecular weight poly(methyl methacrylate) (PMMA) (100 nm total PMMA thickness) was applied to the 4-in. SOI wafer and then exposed at varied e-beam dosage conditions. Through a series of e-beam exposure and resist developing tests, we found that a beam dosage of 900 $\mu C/cm^2$ was required to resolve the 50−300 nm feature sizes. The nanometer dot arrays along with the global and local alignment marks could be written in less than 20 min on a Hitachi HL-700F e-beam writer. While e-beam patterning is generally considered as an academic research tool, and is slow and expensive for most CMOS fabrication processes, the 20 min write time to pattern the limited number of nanometer size dot arrays is economically viable in this mass fabrication process. E-beam lithography gave very good dot size uniformity and accuracy. The stitching error across a 4-in. wafer was found to be only 0.5 μm. Unlike other nanopatterning techniques, for example, nanoimprinting and deep UV lithography, the dot sizes could be easily tailored by redesigning a new e-beam pattern file, while for other nanopatterning methods, expensive molds or masks needed to be remade every time a single feature was modified. It is also very simple to make and register the global and local alignment marks. By writing the alignment marks in the same e-beam lithography step that defined the nanocatalyst spots, we successfully integrated the nano- and microfabrication processes.

After nanopatterning and e-beam resist layer developing (1:3 methyl isobutyl ketone/isopropyl alcohol), a short O_2 plasma descum was performed (150 W, 250 mTorr, 10 s) to clean the wafer prior to metallization. 20 nm Cr or Ti was evaporated on the wafer as barrier layer. 20 nm Ni was deposited on top as CNT growth catalysts by electron beam evaporation. The e-beam resist layer was lifted off in acetone, leaving the catalyst dots deposited at the defined spots on the wafer. The whole wafer was then thoroughly cleaned, rinsed, and dried for microfabrication.

In order for the catalyst seeds that define the CNT locations to survive harsh dry and wet etch chemicals used in microfabrication, we developed catalyst protection schemes before commencing the conventional microfabrication of silicon cantilevers. In general, the protection materials needed to be resistant to dry and wet etch processing chemicals. They also should not interact, reduce, or destroy the catalytic activity of the underlying nanometer sized catalysts. The procedures to put them on and strip them off should be simple enough and compatible with other fabrication process steps. We found that a PECVD Si_3N_4 layer with a thickness of 200 nm worked well for front-side deep reactive ion etching (DRIE). ProTEK chemical series from Brewer Science, Inc., worked best for backside KOH wet etching. 500 Å ProTEK EXP02103-18 etch protectant survived 33% KOH etching at 80 °C for more than 6 h. With these protection materials, the SOI wafer along with the nano-catalysts went through the cantilever microfabrication process without any problems.

The cantilevers were fabricated from SOI wafers through a simple two-mask fabrication process. The front-side mask defined the outline of the cantilevers (cantilever body, cantilever beam, and the tabs that held the cantilevers to the silicon wafer frame). The backside mask shaped the body of the cantilevers. DRIE was used to etch the front-side pattern on the device layer. During the backside silicon etching (KOH wet etching or DRIE), the cantilever beam was thinned down to the SOI oxide layer and stopped (the oxide layer acted as an etching stop). This gave the final

cantilever beam a defined uniform thickness. Each fabrication step was aligned to the global alignment marks that were initially patterned by e-beam lithography. This ensured that the catalyst sites and the final CNTs were located at the exact locations on the cantilever diving boards where they were designed. The process overall layer-by-layer alignment accuracies were found to be within ± 1 μm. Based on the x and y repeating coordinates and the expected stitching and alignment accuracies, we chose to place the catalyst spot at the center of the cantilever beam and 5 μm away from the end of the cantilever diving board.

The most crucial part of the protection scheme was the protection material release step at the end of microfabrication. Several approaches had been investigated to remove the protection layers without reducing and destroying the catalytic activity of the nanometer sized Ni. We found that 6:1 buffered oxide etcher (BOE, 6 parts of 40% NH_4F and 1 part 49% HF) stripped the nitride layer cleanly. ProTEK chemical could be effectively stripped using acetone, followed by methanol and 2-propanol rinsing. The clean catalyst sites were then exposed for wafer scale CNT growth.

We designed and built a homemade 4-in. hot filament direct current PECVD reactor which permitted vast flexibility in process parameter control and monitoring. In addition to normal process variables such as pressure, plasma power, and gas mixture flow and composition, it was possible to also vary the electrode gap, electrode geometry (for angled CNT growth), substrate temperature, and hot filament heating. The reactor was equipped with a residual gas analyzer (RGA), which monitored the relevant gas-phase intermediates important to our growth process.[21]

A formidable challenge for the development of CNT probe tips was the controlled growth of individual isolated CNTs at pre-defined locations on silicon cantilevers that possessed the desired properties (diameter, length, orientation, and crystallinity). We conducted detailed CNT growth studies using high throughput combinatorial methodologies.[22,23] In this case, we found that catalyst spots were positioned at almost the exact locations on fabricated cantilever beams due to accurate process layer-by-layer alignment (accuracy within ± 1 μm). Among the varied catalyst dot sizes, individual CNTs were obtained from 50 to 200 nm catalyst sizes on cantilevers, while 250 and 300 nm catalyst sizes gave multiple CNTs. Using the optimized catalyst formulation (20 nm Cr/Ti and 20 nm Ni) and reactor configurations, the best CNT growth occurred at a gas mixture of 80 sccm NH_3 and 22.5 sccm C_2H_2 at a chamber pressure of 4 Torr, following a hot filament pretreatment (without plasma) with 80 sccm NH_3 for 10 min. Growth of well-aligned individual CNTs occurred at a bias voltage of -550 V (360 W, 690 mA, 800 Ω). To achieve a 3 to 5 μm length of CNT which we found best for AFM imaging, 10 min growth time was needed using the above growth conditions. CNT growth rate was found to be $\sim$550 nm/min, after 1 min induction/nucleation time.

A Hitachi S-4000 scanning electron microscope (SEM) was used to characterize the diameter, length, and orientation of the PECVD-grown CNTs. Figure 2 shows SEM images

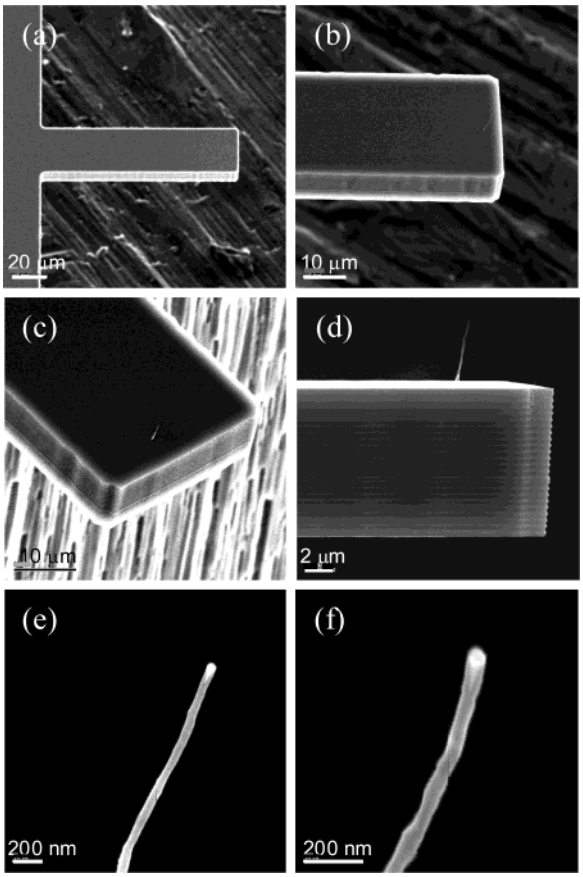

Figure 2. SEM images of CNT AFM cantilever probe tip with an individual CNT grown from a 200 nm catalyst site on a cantilever beam. (a) 45-degree side view with $\times$400 magnification. (b) 45-degree side view with $\times$1000 magnification. (c) 45-degree front view with $\times$1500 magnification. (d) 85-degree side view with $\times$3500 magnification. (e) CNT tip 90-degree side view with $\times$35K magnification. (f) CNT tip 90-degree side view with $\times$70K magnification. One single isolated CNT of 60 nm in tip diameter and 5 μm in length is grown per site from 200 nm catalyst spot size. The CNT is oriented at a 13° angle with respect to the cantilever beam surface normal.

with different angles and zooms of the individual CNT grown from a 200 nm catalyst site on a cantilever beam. As can be seen from these images, only one isolated individual CNT has been grown from this 200 nm catalyst site. The individual CNT is found to be 60 nm in tip diameter and 5 μm in length. The tube axis is tilted 13° toward the front of the diving board end with respect to the cantilever beam surface normal. This 13° angle is required because most commercial AFMs are equipped with tip mounting holders that tilt the cantilevers at 13° relative to the image surface and AFM scanning head. This controlled angle growth is only possible in PECVD where an electric field is applied. As shown in Figure 2e,f, the Ni catalyst is clearly present at the very top of the CNT, indicating that this oriented growth is achieved through a tip growth mechanism. Ni catalyst is wrapped with thin graphite layers at the very top. There is no need to etch away this Ni particle before the CNT tip can be used for imaging.

The desired CNT tip type for AFM imaging applications using this approach is a well aligned and non-entangled

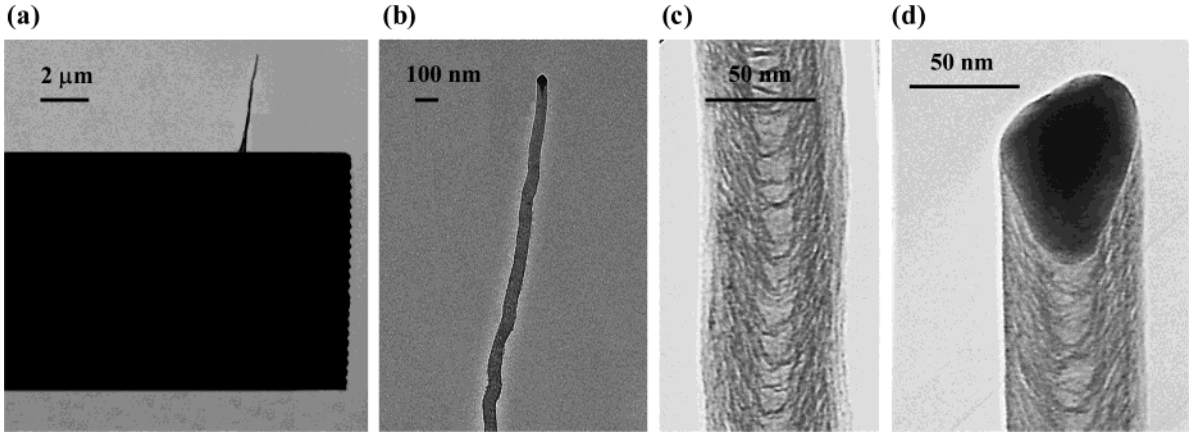

Figure 3. Cross-sectional TEM images of an individual CNT on a cantilever beam with the desired bamboo morphology. (a) CNT cantilever 90-degree side view with ×1500 magnification. The CNT is 60 nm in tip diameter, 5 μm in length, and has a tilt angle of 13° with respect to the cantilever beam surface normal. (b) CNT tip with ×15K magnification. (c) CNT tip body part with ×100K magnification. Multiwall CNT wall structures with bamboo-like periodic crossover parts are clearly visible along the stem. (d) CNT tip end with ×100K magnification. Ni catalyst is wrapped with thin graphite layers at the very end. The clear TEM images here indicate that there is no electron beam induced thermal vibration observed with this 5 μm long CNT.

multiwall carbon nanofiber possessing the bamboo morphology. Changing the PECVD reactor electrode bias influences the CNT growth morphology. We have characterized the CNT growth morphology at various plasma intensities and found that the bamboo morphology occurred at a bias voltage of −550 V (360 W, 690 mA, 800 Ω).[22,23] Increasing the bias to −575 V (400 W, 710 mA, 810 Ω) gave a mixture of CNTs derived from the base growth and tip growth mechanisms. Although the base-growth derived CNTs were more graphitic, they had much poorer vertical alignment than the tip-growth derived CNTs. Therefore we used the bias voltage of −550 V for all our CNT tip growth.

To assess the crystalline quality of the individual CNTs on cantilevers after growth, high-resolution transmission electron microscopy (TEM) analysis was performed. JEOL 2010 TEM was used to image the cross-section of the CNTs using a specially designed chip holder that allowed for direct inspection of the as-grown CNT tips. Figure 3 shows the TEM images of individual CNT on cantilever with the desired bamboo morphology. The individual CNT tip diameter of 60 nm and length of 5 μm are confirmed in these TEM images. From the zoomed-in TEM images (Figure 3c,d), we can clearly observe the multiwall CNT wall structures with bamboo-like periodic crossover parts along the stem. This bamboo morphology is normally achieved in tip growth process at high bias. In fact, because of this unique bamboo morphology, our CNT tips are typically much stiffer than pure multiwall CNTs of the same diameter and length. The clear TEM images in Figure 3 indicate that there was no electron beam induced thermal vibration observed with this 5 μm long CNT. While most pure multiwall CNTs with lengths greater than 3 μm require shortening for AFM imaging,[6−9] we are able to collect satisfactory AFM images using our fabricated CNT tips with lengths as long as 6 μm. Therefore, we can eliminate the shortening step in our process. Furthermore, our as-grown CNT tips with length between 2 and 6 μm are found to be imageable. This reduces the CNT length uniformity requirement for wafer scale individual CNT growth. Our process yield is therefore greatly improved.

Further growth optimization centered on controlling the CNT parameters from the nanometer-sized catalyst spots over the 4-in. wafer scale. Based on SEM and TEM analysis, an assessment of the wafer scale CNT probe tips yield and variations in diameter, length, orientation, and crystallinity has been recorded. Using the optimized catalyst formulation and growth conditions, for released CNT AFM cantilever tips, we have achieved an individual CNT growth yield of 85−90% from 100 to 200 nm catalyst sites. In a typical growth run, the base diameter of an individual CNT probe tip varies from 60 to 80 nm, while the tip diameter varies from 40 to 60 nm. The CNT lengths show a distribution of ±20%. The orientation of individual CNTs on cantilevers varies from 10° to 20° with respect to the cantilever beam surface normal. Our PECVD growth provides mostly bamboo structure CNTs with their crystalline morphologies very similar to the ones demonstrated in Figure 3c,d. Across the wafer, CNT probe tips maintain reasonably consistent diameter, length, orientation, and bamboo morphology. Careful inspection of cantilevers from different areas of the 4-in. wafer has allowed us to analyze statistics for quality control and assurance. We are currently working on further improvement of our process control and yield.

Before we finalized the above fabrication process, we investigated various other approaches for obtaining the desired CNT probe tips. We found growing the CNTs prior to cantilever microfabrication posed many processing challenges due to the inherent mechanical instability of individual CNTs exposed to liquid based processing agents or to CNT protection and stripping chemicals. Preliminary tests showed that upon exposing the as-grown CNTs to photoresist coating and removal or to nitride layer protection and stripping, the CNTs would be heavily damaged or totally removed from the silicon substrate. Since vertical CNT orientation was a prerequisite for obtaining usable tips, growing the CNTs at

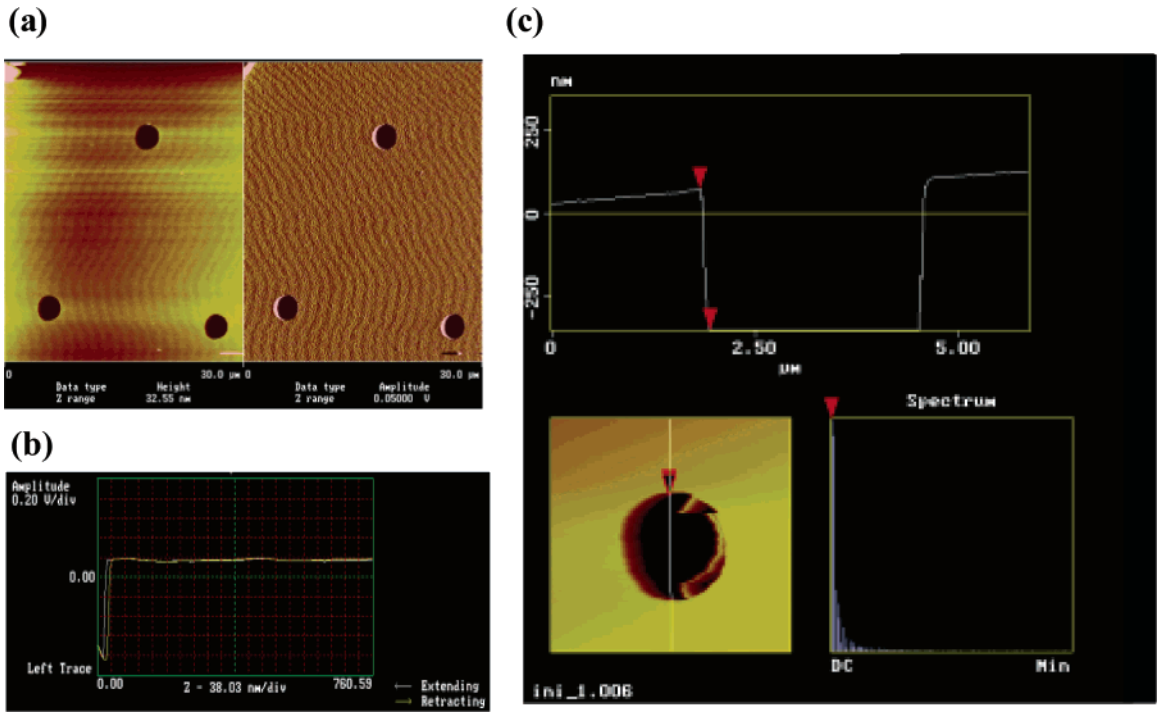

Figure 4. AFM images of an array of 2 μm diameter holes etched 400 nm deep in Si_3N_4 using a CNT AFM probe tip made from this wafer scale fabrication process. (a) A hexagonal array of 2 μm circular holes. (b) The force vs distance curve exhibits well-defined amplitude dampening event characteristic to CNT, indicating a CNT is present. (c) A higher magnification scan of a single hole with the corresponding line cut section analysis.

the end of the fabrication process proved to be a better approach with a reasonable yield of usable CNT tips per wafer. We also found that our wafer-scale catalyst deposition and liftoff steps could not follow cantilever microfabrication. Resist layers must be extremely consistent in this process to yield uniform spot sizes for catalyst deposition, something impossible to achieve on a post-fabricated cantilever wafer. Therefore, we had opted to deposit and protect the catalyst ahead of cantilever fabrication, in predefined diameter and placement on final cantilever beam. This approach seems to be the best option.

It is known that a CNT AFM probe tip is able to fully trace the bottom of the trenches without producing image artifacts.[6,7,9] CNT probe tips can also dramatically improve the imaging resolution and lifetime.[6−9] The image obtained by the conventional silicon tip is limited by its geometry. The micromachined silicon pyramid is physically unable to accurately trace the topographic variations of the surface, especially in critical dimension measurements. Probe tips fabricated from silicon tend to have limited lifetime due to the inherent chemical/mechanical instability of silicon. The silicon tip is brittle, and as such, even when an ultra sharp silicon probe is used for high aspect ratio feature imaging, the tip could easily become worn out or rendered unusable due to mechanical breaking or tip wear. By contrast, the remarkable flexibility of the hexagonal graphitic network allows the CNTs to sustain large distortions via axial compression, such as those encountered with tapping mode imaging.[24,25] Published experimental work has demonstrated that axial deformations are elastic with no atomic defects forming in the hexagonal lattice.[26,27]

It is critical here to perform CNT probe tip evaluation and testing to validate the usefulness of our fabricated CNT probe tips for use in AFM imaging. Commercial AFMs (Digital Instruments Multimode AFM with a Nanoscope IIIA controller and Digital Instruments Dimension 5000 system) were used in our performance tests. The characterization here focused on mechanical stability of the CNT probe tips as they engaged the imaging surface in a conventional AFM operation under tapping mode acquisition. We tested CNT probe tips for continuous scanning for 8 h on hard Si_3N_4 surfaces, and did not observe any tip wear and degradation in lateral resolution. The interaction curves derived from tapping mode imaging (amplitude and deflection signals) were studied to characterize the buckling signature of the CNTs.[6] The force vs distance curve offered an in-situ technique to examine the performance characteristics of the CNT probe tips. Figure 4a shows AFM images of a hexagonal array of 2 μm diameter holes etched 400 nm deep in Si_3N_4 using a CNT AFM probe tip made in this work. Figure 4b exhibits a well-defined amplitude-dampening event that resulted from the CNT AFM probe tip being pushed toward and extracted from the sample surface. The fluctuation in the amplitude vs distance signal indicates the presence of a CNT. Figure 4c shows a higher magnification scan of a single 2 μm hole with the corresponding line cut section analysis. The CNT probe tip is able to fully trace the contour of this circular hole and travel down to the bottom of the hole that is 400 nm deep. The circular hole and its bottom are clearly resolved. This proves that the 5 μm long CNT tip from a flat cantilever beam is stiff enough for routine surface imaging and characterization. We also used a

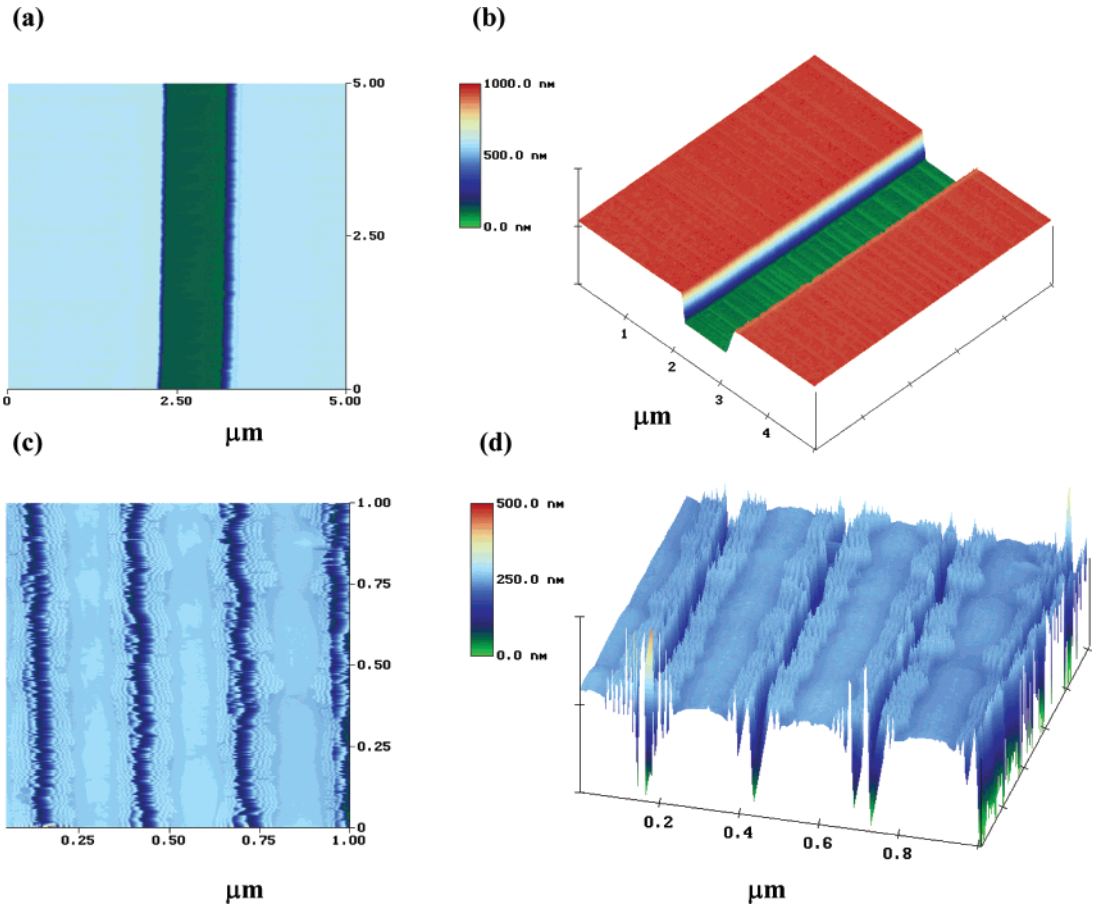

Figure 5. 2D and 3D AFM images of 1 μm and 90 nm trenches using single CNT AFM probe tip made from this work. (a) 2D and (b) 3D AFM images of 1 μm trench. (c) 2D and (d) 3D AFM images of 90 nm trenches. The CNT probe tip is 60 nm in tip diameter and 5 μm in length. It is able to fully resolve the sidewalls and the bottom of the 1 μm trench that is 450 nm deep. The bottom of this 1 μm trench is clearly visible. The 60 nm diameter CNT probe tip is able to fit into the 90 nm trenches and penetrate down to as much as 200 nm in depth. However, the bottom of these 90 nm trenches has not been fully resolved yet.

validation test to determine the number of tip engagements that the CNT could undergo under ambient imaging environment and conditions. We were able to obtain more than 100 tip engagement cycles in air.

We further investigated CNT probe tips made from this wafer-scale fabrication process for AFM critical dimension imaging applications in the semiconductor industry. We tested these CNT tips on photoresist patterned with 1 μm and 90 nm trenches. Figure 5 shows the 2D and 3D AFM images of 1 μm and 90 nm trenches using a CNT probe tip that is 60 nm in tip diameter and 5 μm in length. As seen in Figure 5a,b, the CNT probe tip is able to fully resolve the sidewalls and the bottom of this 1 μm trench that is 450 nm deep. The bottom of the trench is clearly visible. The trench slope angles were measured to be 80 and 69 degrees through the line cut section analysis, very well matched with the resist etching profile characterized by cross-sectional SEM. We then used the same CNT probe tip to characterize the 90 nm trenches. With the perpendicular surface approaching angle during the AFM tapping mode acquisition, the 60 nm diameter CNT probe tip is able to fit into the 90 nm trenches and penetrate down to as much as 200 nm in depth as shown in Figure 5c,d. However, at the current stage, we have not been able to resolve the bottom of these 90 nm trenches yet. Such narrow trenches require CNT probe tips to be less than 20 nm in diameter in order to fully resolve their shapes and bottoms in ambient environment. We are fabricating another batch of wafers for this purpose.

In summary, this study demonstrates a true bottom-up large-scale fabrication methodology for making CNT probe tips for tapping-mode AFM imaging applications. Our wafer scale nanopatterning and integration with silicon microfabrication technologies have proven to be very successful. The catalyst protection and release schemes are effective. The PECVD method enables us to grow well-aligned single CNTs on individual catalyst sites on silicon cantilevers with control over CNT location, diameter, length, and crystallinity. The probe tips made from this method display good image acquisition characteristics. No shortening or post-fabrication treatment is necessary. Preliminary scanning tests show promising imaging capabilities of these tips in critical dimension measurements. Currently the yield of individual CNT growth from 100 to 200 nm catalyst features is about 85−90%. We believe the yield can be quickly ramped to production levels with appropriate engineering of the PECVD chamber and the process quality control and assurance.

Acknowledgment. This material is based upon work supported by the National Science Foundation under Grant No. 0320512 to Integrated Nanosystems, Inc. This work is also supported under NASA contracts No. NAS2-99092 and No. NAS2-03144 to Eloret Corporation and the University of California, Santa Cruz. Chris Huang of KLA-Tencor Corporation is acknowledged for supplying the 1 μm and 90 nm trench samples for this study. The authors thank Dr. Jun Li and Dr. Brett A. Cruden for helpful discussions and Ramsey Stevens for assisting CNT probe tip testing.

References

(1) Dresselhaus, M. S., Dresselhaus, G., Avouris, Ph., Eds.; *Carbon Nanotubes, Topics in Applied Physics*; Springer: Berlin, 2001; Vol. 80.
(2) Li, J.; Lu, Y.; Ye, Q.; Cinke, M.; Han, J.; Meyyappan, M. *Nano Lett.* **2003**, *3*(7), 929.
(3) Li, J.; Ye, Q.; Cassell, A. M.; Ng, H. T.; Stevens, R.; Han, J.; Meyyappan, M. *Appl. Phys. Lett.* **2003**, *82*(15), 2491.
(4) Cassell, A. M.; Ye, Q.; Cruden, B. A.; Li, J.; Sarrazin, P. C.; Ng, H. T.; Han, J.; Meyyappan, M. *Nanotechnol.* **2004**, *15*, 9.
(5) Li, J.; Ng, H. T.; Cassell, A. M.; Fan, W.; Chen, H.; Ye, Q.; Koehne, J.; Han, J.; Meyyappan, M. *Nano Lett.* **2003**, *3*(5), 597.
(6) Dai, H.; Hafner, J. H.; Rinzler, A. G.; Colbert, D. T.; Smalley, R. E. *Nature* **1996**, *384*, 147.
(7) Nguyen, C. V.; Chao, K.; Stevens, R. M.; Delzeit, L.; Cassell, A.; Han, J.; Meyyappan, M. *Nanotechnol.* **2001**, *12*, 363.
(8) Nguyen, C. V.; So, C.; Stevens, R. M.; Li, Y.; Delzeit, L.; Sarrazin, P.; Meyyappan, M. *J. Phys. Chem. B* **2004**, *108*, 2816.
(9) Nguyen, C. V.; Stevens, R. M. D.; Barber, J.; Han, J.; Meyyappan, M. *Appl. Phys. Lett.* **2002**, *81*, 901.
(10) Wong, S. S.; Harper, J. D.; Lansbury, P. T., Jr.; Lieber, C. M. *J. Am. Chem. Soc.* **1998**, *120*, 603.
(11) Nishijima, H.; Kamo, S.; Akita, S.; Nakayama, Y. *Appl. Phys. Lett.* **1999**, *74*, 4061.
(12) Stevens, R. M.; Nguyen, C. V.; Meyyappan, M. *IEEE Trans. Nanobiosci.* **2004**, *3*, 56.
(13) Wong, S. S.; Joselevich, E.; Woolley, A. T.; Cheung, C. L.; Lieber, C. M. *Nature* **1998**, *394*, 52.
(14) Wong, S. S.; Woolley, A. T.; Joselevich, E.; Cheung, C. L.; Lieber, C. M. *J. Am. Chem. Soc.* **1998**, *120*, 8557.
(15) Stevens, R.; Nguyen, C.; Cassell, A.; Delzeit, L.; Meyyappan, M.; Han, J. *Appl. Phys. Lett.* **2000**, *77*, 3453.
(16) Hafner, J. H.; Cheung, C. L.; Lieber, C. M. *Nature* **1999**, *398*, 761.
(17) Hafner, J. H.; Cheung, C. L.; Lieber, C. M. *J. Am. Chem. Soc.* **1999**, *121*, 9750.
(18) Cheung, C. L.; Hafner, J. H.; Lieber, C. M. *PNAS* **2000**, *97*, 3809.
(19) Franklin, N. R.; Li, Y.; Chen, R. J.; Javey, A.; Dai, H. *Appl. Phys. Lett.* **2001**, *79*, 4571.
(20) Yenilmez, E.; Wang, Q.; Chen, R. J.; Wang, D.; Dai, H. *Appl. Phys. Lett.* **2002**, *80*, 2225.
(21) Cruden, B. A.; Cassell, A. M.; Ye, Q.; Meyyappan, M. *J. Appl. Phys.* **2003**, *94*(6), 4070.
(22) Cassell, A. M.; Ye, Q.; Cruden, B. A.; Li, J.; Sarrazin, P. C.; Ng, H. T.; Han, J.; Meyyappan, M. *Nanotechnol.* **2004**, *15*, 9.
(23) Cassell, A. M.; Ng, H. T.; Delzeit, L.; Ye, Q.; Li, J.; Han, J.; Meyyappan, M. *Appl. Catal. A: General* **2003**, *254*, 85.
(24) Lee, S. I.; Howell, S. W.; Raman, A.; Reifenberger, R.; Nguyen, C. V.; Meyyappan, M. *Nanotechnol.* **2004**, *15*, 416.
(25) Yu, M. F.; Kowalewski, T.; Ruoff, R. S. *Phys. Rev. Lett.* **2000**, *85*, 1456.
(26) Hertel, T.; Martel, R.; Avouris, Ph. *J. Phys. Chem. B* **1998**, *102*, 910.
(27) Ruoff, R. S.; Qian, D.; Liu, W. K. *C. R. Phys.* **2003**, *4*, 993.

NL049341R